

Anatomical features of plantar aponeurosis: cadaveric study using ultrasonography and magnetic resonance imaging

Clarissa Canella Moraes do Carmo ·
Lina Isabel Fonseca de Almeida Melão ·
Marcio Freitas Valle de Lemos Weber · Debra Trudell ·
Donald Resnick

Received: 6 January 2008 / Revised: 4 March 2008 / Accepted: 19 March 2008 / Published online: 25 June 2008
© ISS 2008

Abstract

Objective Abnormalities of the plantar aponeurosis are commonly encountered in patients with subcalcaneal heel pain. Understanding normal anatomy is required to accurately diagnose some disorders of the foot. The purpose of our study was to describe the normal anatomy of the plantar aponeurosis, using ultrasonography and MRI with close anatomic correlation in cadavers.

Materials and methods After MRI and ultrasonography of 10 cadaveric foot specimens, the thickness of the central and lateral portions of the plantar aponeurosis displayed by imaging studies was measured by three radiologists. One specimen was sectioned in the transverse plane, one in the coronal plane, one in the sagittal plane, and two in a sagittal oblique plane. Normal anatomy was identified and similar measurements of the plantar aponeurosis were also made. An average value was determined and a statistical analysis was accomplished.

Results The calcaneal insertions of the plantar aponeurosis were better visualized than its distal portions with both MRI and ultrasonography. The measurements of the plantar aponeurosis made by three different radiologists were

different, but without statistical significance. The average measurements for the central and lateral portions of the plantar aponeurosis with both imaging methods were different from each other because of differences in the morphology of these structures. The values obtained with ultrasonography and MRI, were also different from each other for both the central and lateral portions of the plantar aponeurosis, but with no statistical significance.

Conclusions We have described the detailed anatomy of the plantar aponeurosis with emphasis on the more distal structures that can be visualized with MRI. There was no statistically significant difference between the accuracy of ultrasonography and MRI regarding the measurements of the thickness of the central and lateral portions of the plantar aponeurosis. Knowledge of the normal anatomy of these structures enables the radiologist to identify early alterations, providing timely diagnosis and treatment.

Keywords Plantar · Aponeurosis · Musculoskeletal

Introduction

Abnormalities of the plantar aponeurosis are commonly encountered in patients with subcalcaneal heel pain. Understanding normal anatomy is required to accurately diagnose some disorders of the foot including plantar fasciitis, which may affect up to 10% of running athletes. The plantar aponeurosis is important functionally because it has been shown to be the most important structure providing dynamic longitudinal arch support in the foot.

The purpose of our study is to describe the normal anatomy of the plantar aponeurosis, using ultrasonography and MRI, with further close anatomic correlation in cadavers.

C. C. Moraes do Carmo · L. I. Fonseca de Almeida Melão ·
M. F. Valle de Lemos Weber · D. Trudell · D. Resnick
Department of Radiology, UCSD,
200 West Arbor Drive,
San Diego, CA 92103, USA

C. C. Moraes do Carmo (✉) · L. I. Fonseca de Almeida Melão ·
M. F. Valle de Lemos Weber · D. Trudell · D. Resnick
VA Healthcare System San Diego,
3350 La Jolla Village Drive,
La Jolla, CA 92161, USA
e-mail: clacanella@yahoo.com.br

Materials and methods

Cadaveric specimen preparation

Ten foot specimens were harvested from 10 non-embalmed cadavers (5 right and 5 left feet) and were derived from legs cut through the distal portions of the tibia and fibula. The specimens were fixed in a neutral position, and immediately deep frozen at -40°C for at least 24 h (Forma BioFreezer; Forma Scientific, Marietta, OH, USA).

Cadaveric ultrasonography and MRI

All 10 cadaveric specimens were later thawed prior to imaging. Ultrasonography was performed using a 12.5-MHz linear transducer in a Philips IU22 machine. The specimens were positioned simulating the prone patient's position. A thick layer of ultrasound gel was used because of the superficial position of the plantar aponeurosis. Images of the specimens in the sagittal and coronal planes were made with the probe perpendicular to the plantar aponeurosis to avoid artifacts that reduce the echogenicity of the plantar aponeurosis tissue. The central portion was visualized from its

attachments at the posterior portion of the medial tuberosity of the calcaneus to its division into five fascicles. The lateral portion was identified from its attachments at the lateral portion of the medial tuberosity of the calcaneus to its division into two fascicles. The medial portion of the plantar aponeurosis was not visualized. All the scans were reviewed by three radiologists at different times. The thickness of the plantar aponeurosis was measured 1 cm distal to its attachment at the calcaneus for both the central and lateral portions.

After ultrasonography, MRI was performed in a 1.5-T MR imager (GE 1.5 T Signa Excite HTDX) with an extremity quadrature coil (Invivo). The MRI protocol consisted of T1-weighted spin-echo sequences (TR=500, TE=12) with a slice thickness of 1.5 mm and a gap of 0.5 mm. The field of view was 10 cm in the coronal plane, 16 cm in the sagittal plane, and 18 cm in the axial and sagittal oblique planes. The sagittal oblique plane was performed parallel to the peroneus brevis tendon for better analysis of the lateral fascicle of the plantar aponeurosis. The data acquisition matrix was 320×256 pixels. The NEX was 2 and the band width was 22.73. Measurements of the plantar aponeurosis were also performed 1 cm distal to its

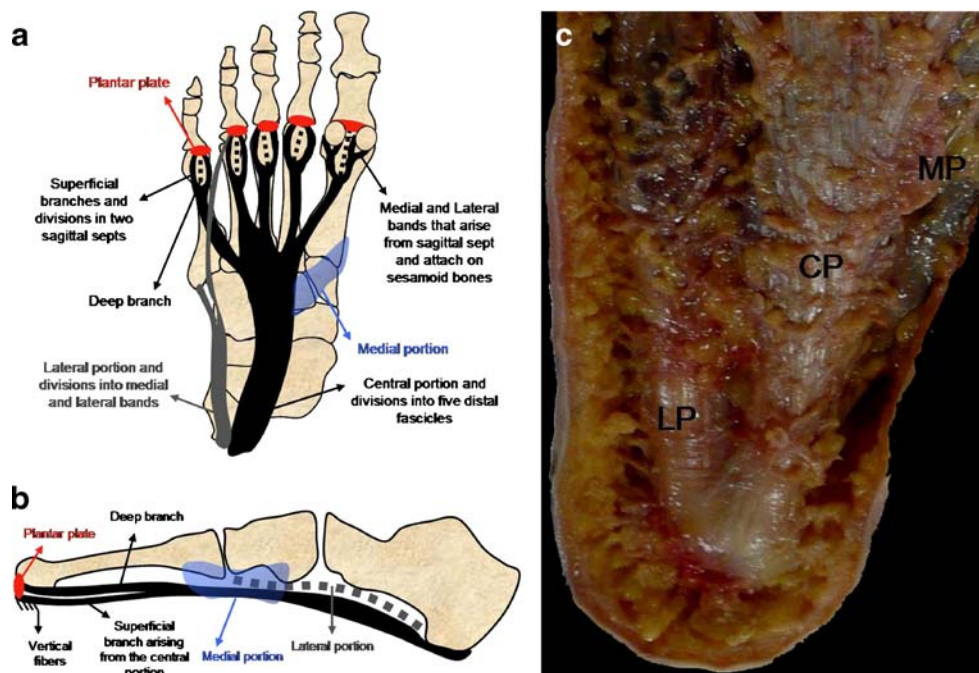
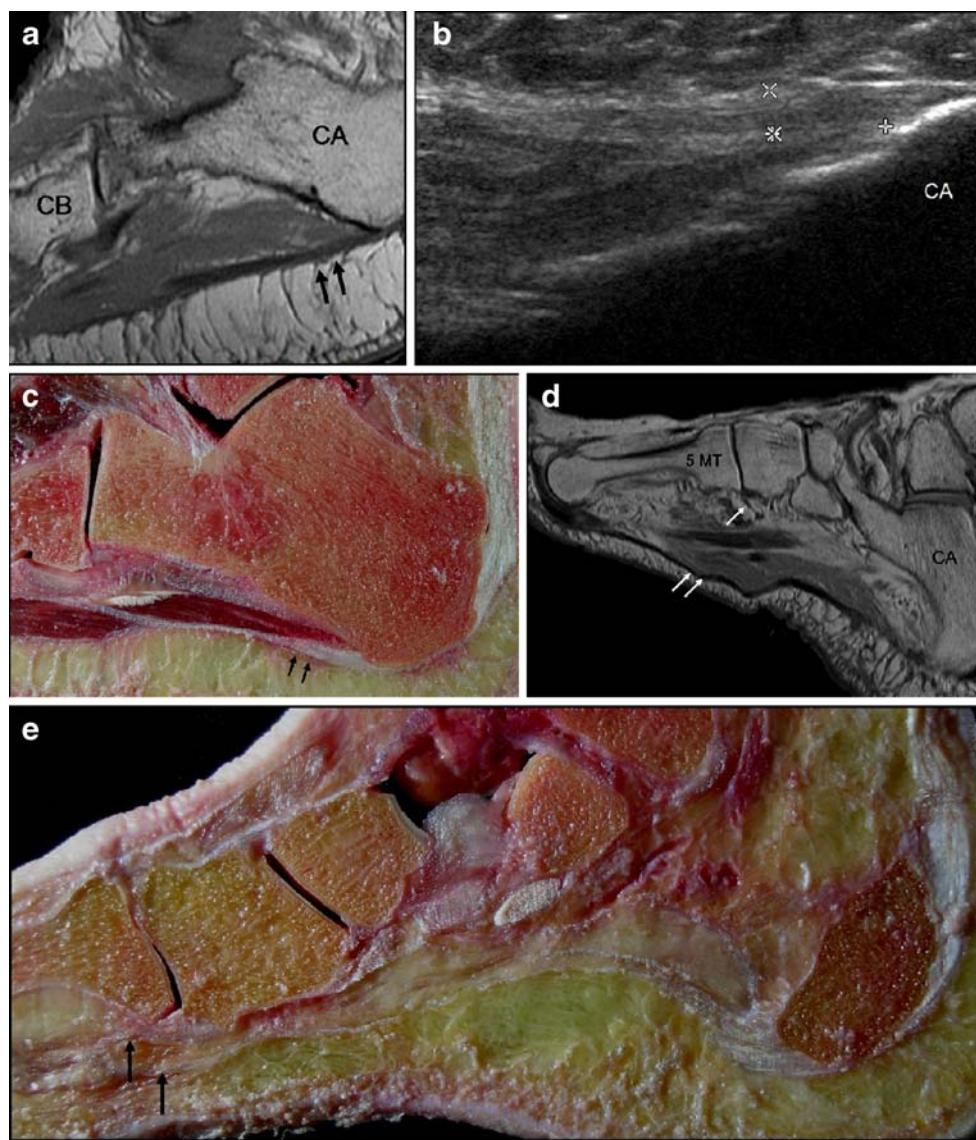


Fig. 1 **a** Axial view of the plantar aponeurosis showing the central portion (*in black*) of the plantar aponeurosis attaching to the posterior aspect of the medial tuberosity of the calcaneus, and its five distal divisions, superficial and deep branches (*dotted lines*) that attach to the plantar plate (*in red*) of the second to fifth toes. In the toes, the medial and lateral bands of the superficial branch attach to the sesamoid bones and plantar plate (*in red*). The lateral portion (*in gray*) of the plantar aponeurosis arises from the lateral aspect of the medial tuberosity of the calcaneus and its distal medial and lateral bands attach to the plantar plate of the fourth toe and to the base of the fifth

metatarsal respectively. The medial portion (*in blue*) of the plantar aponeurosis covers the fascia of the abductor hallucis muscle medially and is continuous with the dorsal aponeurosis laterally. **b** Sagittal view of the plantar aponeurosis showing the central (*in black*), the lateral (*in gray*), and the medial (*in blue*) portions of the plantar aponeurosis. Note also the vertical fibers (*distal thin black lines*) that arise from the sagittal bands and attach into the skin. **c** Dissected specimen showing the central (CP), lateral (LP), and medial (MP) portions of the plantar aponeurosis

Fig. 2 a Sagittal oblique T1-weighted SE MRI (500/12, 320×256 matrix, 18-cm field of view) showing the lateral portion of the plantar aponeurosis, which measures 3.6 mm (*black arrows*), 1 cm distal to the attachment at the calcaneus. **b** Ultrasonography showing the lateral portion of the plantar aponeurosis (*white markers*), which measures 4.1 mm, 1 cm distal to the attachment at the calcaneus. **c** Corresponding anatomic slice of **a** and **b**. **d** Sagittal oblique T1-weighted SE MRI (500/12, 320×256 matrix, 18-cm field of view) of another specimen showing the medial (*double white arrows*) and lateral (*white arrow*) bands of the lateral portion of the plantar aponeurosis distally. **e** Structures shown on **d** can also be visualized in the gross specimen (*black arrows*). CA, calcaneus; CB, cuboid; 5 MT, fifth metatarsal



attachment to the calcaneus by three radiologists at different times, as was done with the ultrasonography images.

Cadaveric specimens sections

After ultrasonography and MRI, all cadaveric specimens were frozen again at -40°C for at least 24 h; according to the quality of the ultrasonographic and MR images, 1 of the 10 specimens was sectioned transversely, 1 in the coronal plane, 1 in the sagittal plane, and 2 in the sagittal oblique plane, into 3-mm thick slices corresponding to the imaging planes. The other five specimens were used in another anatomic project. Also, 1 additional specimen was dissected by two musculoskeletal radiologists and an orthopedic surgeon. All specimens were photographed by a digital camera. Measurements of the central and lateral portions of the plantar aponeurosis were made in anatomic sections in 5 specimens, and these measurements were considered our

gold standard. A statistical analysis of the measurements was carried out for ultrasonography, MRI, and gold standard measurements with an analysis of variance test (ANOVA) and the Pearson correlation method.

Results

General anatomy

The plantar aponeurosis is divided into central, lateral, and medial portions. The central portion is the thickest, attaches at the posterior aspect of the medial tuberosity of the calcaneus posterior to the origin of the flexor digitorum brevis tendon, and is 1.5 to 2.0 cm in width [1]. This portion of the plantar aponeurosis medially covers the flexor digitorum longus muscle, blending the dorsal aponeurosis, and laterally borders the lateral sulcus of the

Fig. 3 **a** Coronal T1-weighted SE MRI (500/12, 320×256 matrix, 10-cm field of view) showing the central (*double black arrows*), medial (*white arrow*), and lateral (*black arrow*) portions of the plantar aponeurosis covering the superficial flexor digiti minimi brevis, abductor hallucis, and abductor digiti minimi muscles respectively. **b** Coronal T1-weighted SE MRI (500/12, 320×256 matrix, 10-cm field of view), more distal than **a**, showing the distal fascicles (*black arrows*) of the central portion of the plantar aponeurosis and the deep branch (*white arrow*) that derives from each of the five fascicles and embraces the flexor tendons. **c** Correlated gross specimen sectioned in the same plane as **a**. **d** Correlated gross specimen sectioned in the same plane as **b**. ADMM, abductor digiti minimi muscle; SFDMM, superficial flexor digiti minimi brevis muscle; AHM, abductor hallucis muscle; 1 MT, first metatarsal; 2 MT, second metatarsal; 3 MT, third metatarsal; FT, flexor tendons

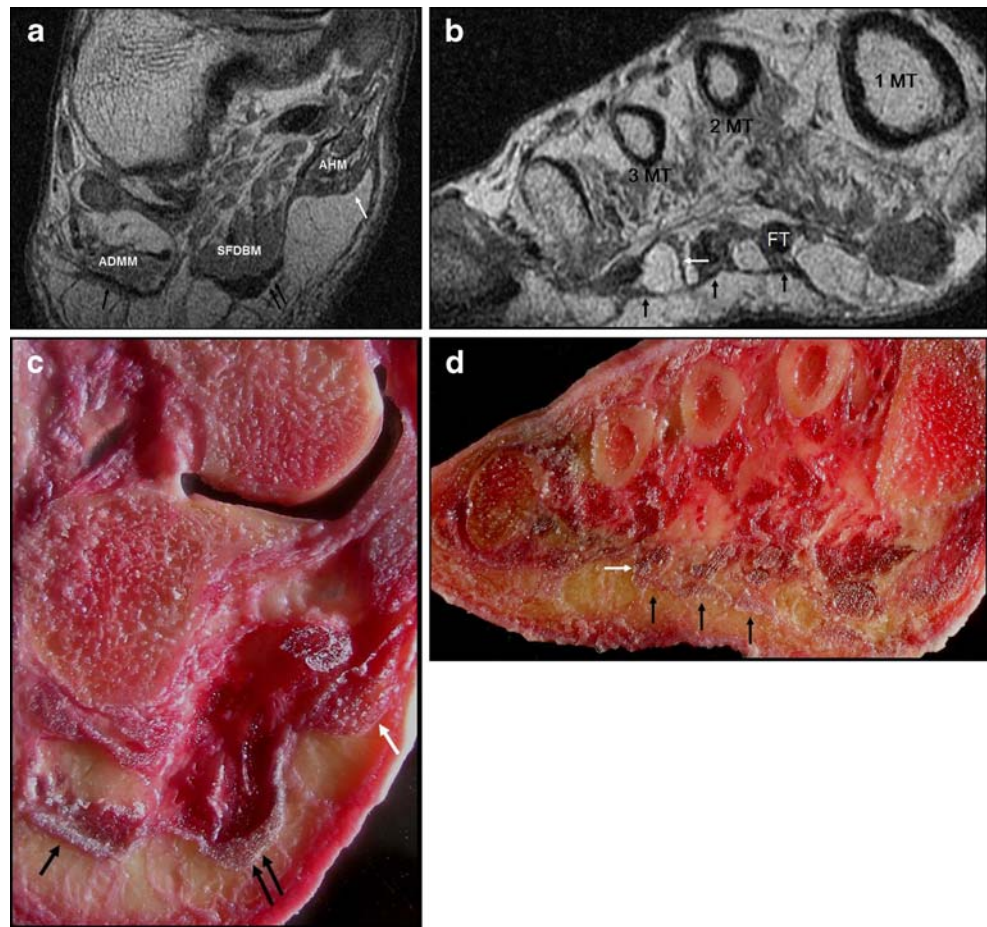


Table 1 Average measurements of the central and lateral portions of the plantar aponeurosis by three radiologists using ultrasonography and MRI—correlation with gross specimens

Specimen	CF	CF	CF	LF	LF	LF
	USG (mm)	MRI (mm)	GS (mm)	USG (mm)	MRI (mm)	GS (mm)
1	4.5	7.6	—	3.7	6.3	—
2	4.2	4.3	3.8	3.3	4.4	3.0
3	4.9	4.8	—	3.0	4.0	—
4	3.2	4.9	4.5	2.8	5.1	3.0
5	3.7	4.7	—	2.9	4.2	—
6	3.5	3.1	—	2.4	2.8	—
7	3.3	3.4	3.3	2.7	2.6	1.8
8	4.7	3.7	6.6	3.0	3.9	3.0
9	3.3	5.3	—	3.5	3.6	—
10	3.5	4.4	4.1	4.1	3.6	3.1
Average measurement	3.8	4.6	4.4	3.1	4.0	2.7

CF, central fascia; USG, ultrasonography; GS, gross specimen; LF, lateral fascia

plantar aponeurosis (Fig. 1). Distally, at the level of the metatarso-phalangeal joints, the central portion of the plantar aponeurosis divides into five fascicles, one for each of the toes [2]. Each fascicle divides into superficial and deep branches (see Fig. 3). The deep branch inserts at the metatarso-phalangeal joints. The superficial branch sends fibers to the natatory ligament and divides into two sagittal septa that embrace the flexor tendon of each toe, blending with their sheaths [2]. In the second, third, fourth, and fifth digits these sagittal septa insert onto the plantar plate, interosseous ligament, and deep transverse metatarsal ligament. In the big toe, the sagittal septum divides into lateral and medial bands that insert onto the plantar plate and sesamoid bones. Both sagittal septa are continuous with some vertical fibers that insert into the skin [1, 3].

The lateral portion of the plantar aponeurosis attaches onto the lateral aspect of the medial process of the calcaneus covering the surface of the abductor digiti quinti muscle, is 1.0 to 1.5 cm in width [1] and, in common with the central portion, is thick posteriorly and thin anteriorly (Fig. 2). This portion of the plantar aponeurosis is continuous medially with the central portion and laterally with the dorsal fascia [1, 2]. Distally, it divides in two bands, a medial band that turns around

the abductor digiti minimi muscle and inserts onto the plantar plate of the third and sometimes fourth metatarsophalangeal joints, and a lateral band that inserts onto the base of the fifth metatarsal and becomes the metatarsoscapho-ligament [1, 2].

The medial portion of the plantar aponeurosis is thin, attaches behind to the lacinate ligament, and covers the surface of the abductor hallucis longus muscle (Figs. 1, 3). This portion of the plantar aponeurosis is continuous medially with the dorsal fascia and laterally with the central portion of the plantar aponeurosis [1].

Ultrasonography imaging

When imaged with ultrasonography at 90° with the axial plane of the foot, the central and lateral portions of the normal plantar aponeurosis are homogeneous and hyperechoic, with a striated appearance that resulted from the longitudinal orientation of its fibers. The calcaneal insertions of the plantar aponeurosis were better visualized than its distal portions. We were able to identify the insertion of the central and lateral fascicles of this structure at the medial tuberosity of the calcaneus and the more distal portions of the plantar aponeurosis up to the level of the cuboid bone (Figs. 2, 4). More distal structures were not visualized.

The measurements of the central and lateral portions of the plantar aponeurosis with ultrasonography, MRI, and the gross specimens are shown in Table 1.

Magnetic resonance imaging

All three portions of the plantar aponeurosis and the perifascial structures could be visualized with high resolution MRI in all three imaging planes, better in the sagittal than in the axial plane. On the T1-weighted images, the three components of the plantar aponeurosis had low signal intensity in all imaging planes with a striated appearance and a band-like shape [4–6].

With regard to the central portion, its division into five fascicles appeared as diverging cord-like structures of low signal intensity in the axial and coronal planes. The superficial and deep branches of these fascicles were seen in the coronal plane as thin serpentine-like structures of low signal intensity arising from the distal plantar aponeurosis. The two sagittal septa that are derived from each superficial branch and the vertical fibers that connect the septum into the skin were not visualized (Figs. 3, 4 and 5).

Discussion

To date, there have been many articles describing the normal anatomy of the plantar aponeurosis, but most of

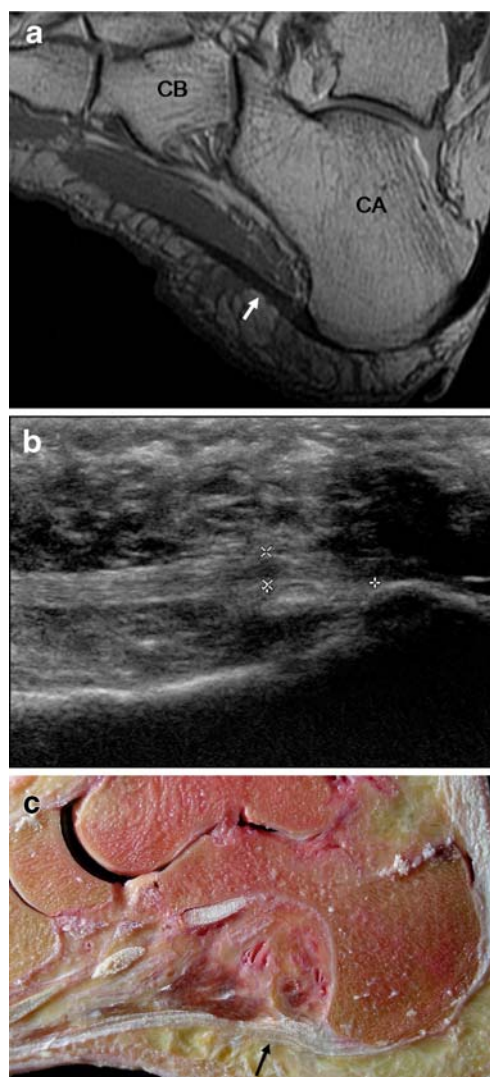
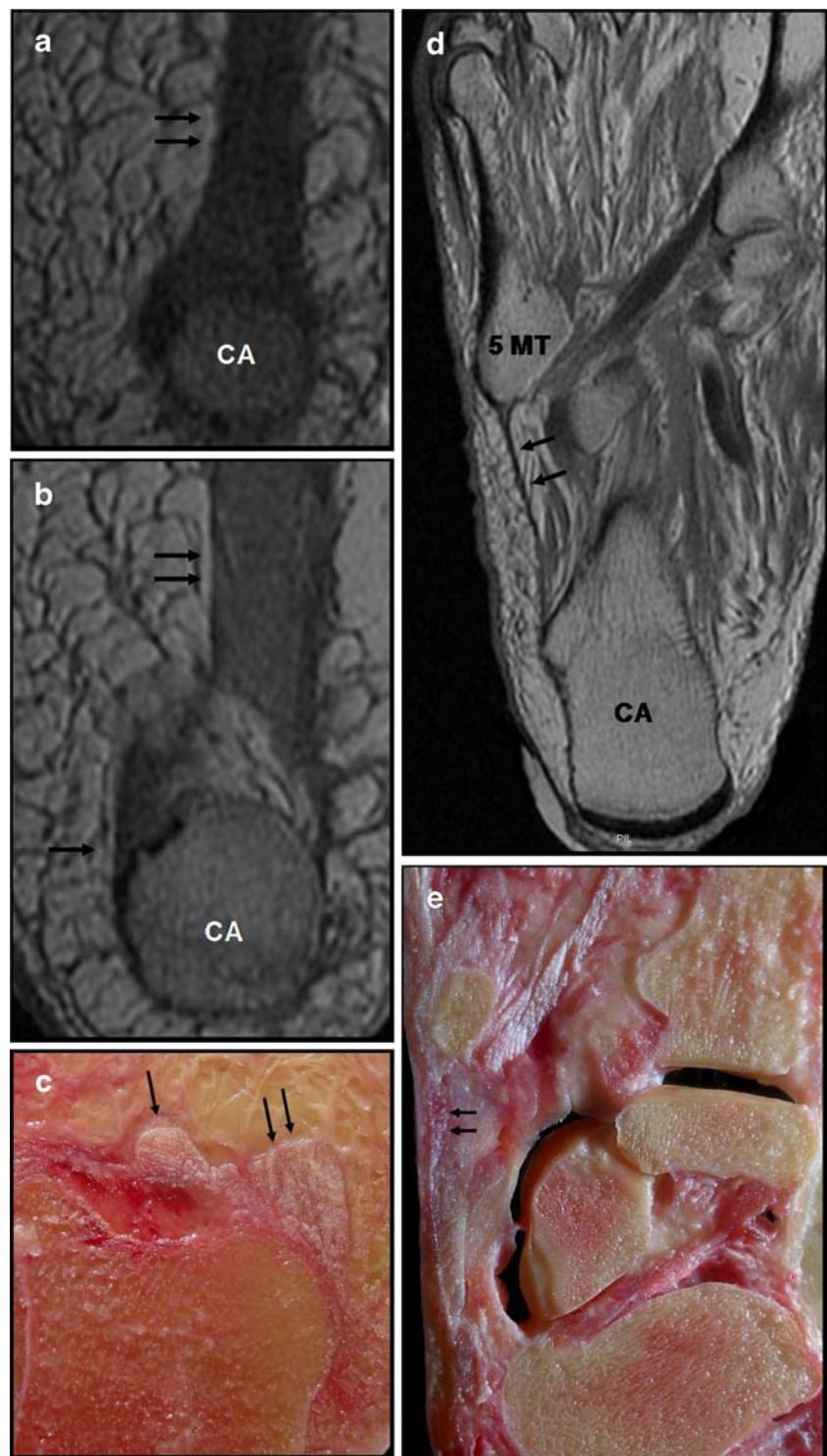


Fig. 4 **a** Sagittal T1-weighted SE MRI (500/12, 320×256 matrix, 16-cm field of view) showing the central portion of the plantar aponeurosis, which measures 3 mm (*white arrow*). **b** Ultrasonography in a sagittal plane showing the central portion of the plantar aponeurosis, which also measures 3 mm (*white markers*). **c** Corresponding anatomic slice of **a** and **b** showing the central portion of the plantar aponeurosis, which measures 6 mm (*black arrow*). CA, calcaneus; CB, cuboid

these describe the attachment of this structure to the calcaneus. Hicks and co-workers [7] described the distal attachment of the plantar aponeurosis as a very strong structure. This finding was confirmed in our study, documenting the anatomic complexity of the components at the distal part of the plantar aponeurosis. Berkowitz et al. [8] and Cardinal et al. [9] described the aponeurosis as a homogeneous and hyperechoic structure, with a striated appearance on ultrasonography. With MRI, Theodorou and co-workers [10, 11] described the three components of the plantar aponeurosis revealing low signal intensity with a striated appearance and a band-like shape, similar to the results of our study. Gibbon and Long [12] and Cardinal et

Fig. 5 **a** Axial T1-weighted SE MRI (500/12, 320×256 matrix, 10-cm field of view) showing the central (*double black arrows*) portion of the plantar aponeurosis arising from the posterior aspect of the medial tuberosity of the calcaneus. **b** Axial T1-weighted SE MRI (500/12, 320×256 matrix, 10-cm field of view) showing the lateral portion of the plantar aponeurosis arising from the lateral aspect of the medial tuberosity (*black arrow*). **c** Correlating the anatomic slice in **a** and **b**. **d** Axial T1-weighted SE MRI (500/12, 320×256 matrix, 16-cm field of view) showing the lateral band (*black arrows*) of the lateral portion of the plantar aponeurosis attaching to the base of the fifth metatarsal. This structure forms the metatarsal-calcaneus ligament. **e** Correlating the anatomic slice in **d**. CA, calcaneus; 5 MT, fifth metatarsal



al. [9] indicated that ultrasonography provided a very good assessment of the plantar aponeurosis.

Regarding the thickness of the central portion of the plantar aponeurosis, the average value obtained in our study was 4.2 mm with ultrasonography. In the study by Balint and co-workers [13] this value, also with ultrasonography, was similar to ours (4.4 mm). In two additional articles [8, 9],

these values were lower than those obtained in our study—3.2 and 2.6 mm respectively. These differences probably relate to the fact that the measurement of the plantar aponeurosis was made 10 mm distal to the calcaneal attachment, different from the technique described by other authors [12, 14]. We chose this technique because we thought that this region of the plantar aponeurosis is the site at which the ma-

jority of lesions occur in cases of plantar fasciitis and plantar fascial rupture [10, 11]. We were not able to find a description of measurements of the lateral portion of the plantar aponeurosis in the available literature, although we are not certain of the clinical importance of lesions of this structure.

There are some important comments regarding the statistical analyses of the measurements of the central and lateral portions of the plantar aponeurosis. First, in our study, these measurements were made by three different radiologists and the resulting values were different, but without statistical significance. Second, there were no statistically significant differences between the values related to gender and age of the specimens. Third, the average measurements for the central and lateral portions of the plantar aponeurosis were different from each other for both ultrasonography and MRI; and the reasons for these findings were not clear. Finally, the values obtained with ultrasonography and MRI were different from each other for both the central and lateral portions of the plantar aponeurosis. Comparing these values with the gold standard, derived from measurement of anatomic specimens, we noticed that according to the inter-test of variability, the variability of values with MRI (central portion 30%, lateral portion 17%) was a little higher than with ultrasonography (central portion 22%, lateral portion 16%), but with no statistical significance. This means that we did not document significant differences in the accuracy of these methods, even with the better anatomic definition provided by MRI. Variations like this can occur when studying a very small and thin structure such as the distal portions of the plantar aponeurosis. According to this fact, Brushoj et al. [15] investigated the reproducibility of measurements of the tendons of the ankle using ultrasonography and MRI and described the variability of the values as being higher for small tendons such as the tibialis anterior and posterior than for larger tendons such as the Achilles tendon. To date, there have been no articles published comparing the measurements obtained with ultrasonography and MRI of the central and lateral portions of the plantar aponeurosis.

Our study has some limitations, including the small number of specimens and the absence of histopathologic correlation. We did not measure the thickness of the plantar aponeurosis in all specimens because 5 of the 10 specimens in the study were used for another anatomic project. We did not use an oblique plane to better visualize the medial portion of the plantar aponeurosis because it was well demonstrated in the sagittal plane. Clinical information such as previous foot disorders and surgery was not available. Artifacts produced by freezing and thawing of the specimens may have influenced the measurements and the structures analyzed, although these artifacts appeared to be a minor problem, as described by Muhle and co-workers

[16]. Finally, further study of a patient population without plantar disorders would be useful to complement the data derived from our study.

We have described the detailed anatomy of the plantar aponeurosis with emphasis on the more distal structures that can be visualized with MRI. There was no statistically significant difference between the accuracy of ultrasonography and MRI regarding the measurements of the thickness of the central and lateral portions of the plantar aponeurosis. Knowledge of the normal anatomy of these structures enables the radiologist to identify early alterations, providing timely diagnosis and treatment.

Acknowledgements The authors would like to express their gratitude to Paul Clopton for the statistical support.

References

1. Sarrafian S. Plantar aponeurosis. In: Sarrafian S, editor. *Anatomy of the foot and ankle: descriptive, topographic, and functional*. 2nd ed. Philadelphia: Lippincott; 1993. p. 137–149.
2. Warwick R, Williams P, editors. *Gray's anatomy of the human body*. 35th British ed. Philadelphia: Saunders; 1973. p. 579–580.
3. Bojsen-Møller F, Flagstad K. Plantar aponeurosis and internal architecture of the ball of the foot. *J Anat* 1976; 121: 599–611.
4. Resnick D. Abnormalities of the plantar soft tissues. In: Resnick D, editor. *Diagnosis of bone and joint disorders*. 3rd ed. Philadelphia: Saunders; 1995. p. 3204–3208.
5. Resnick D, Kang H, Pretterklieber M. *Internal derangements of joints*, vol 1. Amsterdam: Elsevier; 2007. p. 129–152.
6. Resnick D, Kang H, Pretterklieber M. *Internal derangements of joints*, vol 2. Amsterdam: Elsevier; 2007. p. 1218–1419.
7. Hicks J. The mechanics of the foot: the plantar aponeurosis and the arch. *J Anat* 1954; 88: 25–31.
8. Berkowitz JF, Kier R, Rudicel S. Plantar fasciitis: MR imaging. *Radiology* 1991; 179: 665–667.
9. Cardinal E, Chem R, Beauregard G, et al. Plantar fasciitis: sonographic evaluation. *Radiology* 1996; 201: 257–259.
10. Theodorou DJ, Theodorou SJ, et al. Disorders of the plantar aponeurosis: a spectrum of MR imaging findings. *AJR Am J Roentgenol* 2001; 176: 97–104.
11. Theodorou DJ, Theodorou SJ, Kakitsubata Y, et al. Plantar fasciitis and fascial rupture: MR imaging findings in 26 patients supplemented with anatomic data in cadavers. *Radiographics* 2000; 20: S181–S197.
12. Gibbon W, Long G. Ultrasound of the plantar aponeurosis (fascia). *Skeletal Radiol* 1999; 28: 21–26.
13. Balint PV, Kane D, Wilson H, McInnes IB, Sturrock RD. Ultrasonography of enthesal insertions in the lower limb in spondyloarthropathy. *Ann Rheum Dis* 2002; 61: 905–910.
14. Griffith JF, Wong TY, et al. Sonography of plantar fibromatosis. *AJR Am J Roentgenol* 2002; 179: 1167–1172.
15. Brushoj C, Henriksen BM, Albrecht-Beste E, Hölmich P, Larsen K, Nielsen MB. Reproducibility of ultrasound and magnetic resonance imaging measurements of tendon size. *Acta Radiol* 2006; 47 9: 954–959.
16. Muhle C, Frank LR, Rand T, et al. Collateral ligaments of the ankle: high-resolution MR imaging with a local gradient coil and anatomic correlation in cadavers. *Radiographics* 1999; 19: 673–683.